Research Article Vol. 3, No. 3 / 15 Mar 2024 / Optics Continuum 441
OPTICS CONTINUUM

Optical force propelled by metamaterial surface waves excitation: pushing and tractor beam sources

VIVIAN GRUNHUT[1,2] AND MAURO CUEVAS[1,2,*]

[1]Consejo Nacional de Investigaciones Científicas y Técnicas (CONICET), Buenos Aires, Argentina
[2]Facultad de Ingeniería-LIDTUA-CIC, Universidad Austral, Mariano Acosta 1611, Pilar 1629, Buenos Aires, Argentina
[*]mcuevas@austral.edu.ar

Abstract: Theoretical research on opto–mechanical interactions at sub–wavelength levels using surface waves (SWs) excitation has a great impact in both the academic knowledge and practical realm. In this letter we have revealed that the dynamic characteristics of the SWs excited along a metamaterial boundary, such as its forward or backward propagation nature, provide a direct demonstration about the direction of action of the optical force exerted on a dielectric nano–particle. In particular, by using a rigorous electromagnetic formalism based in the second Green identity, we have modeled the scattering problem of a Gaussian beam impinging on a metamaterial plane surface with a sub–wavelength localized defect. We have shown that depending on the nature of the excited SW, dielectric nano–particles placed near the surface can be pushed away or towards the localized defect. We believe that this work unveils the potential implementation of sub–wavelength defects as sources of pushing or pulling optical forces.

1. Introduction

Due to the unique property of high confinement that allowed optics to develop at sub–wavelength level, excitation of surface waves (SWs) –electromagnetic waves propagating along the interface between media with opposite signs of their permittivities or permeabilitties– became a subject of great interest in science applications. The vast majority of research in the last century was focused on SWs with *p* polarization, taking place in the visible range, that occurs at the interface separating a conventional dielectric medium, such as an insulator medium with positive permittivity, from a metallic medium, with negative permittivity [1].

Perhaps one of the most interesting applications of metallic SWs refers to the optical control of the movement of nano–particles by exchanging momentum with light. Since the propagation constant of the SW at the insulator–metal interface is grater than that of the photon in the insulator medium, where the nano–particle is placed (usually vacuum or water), the momentum imparted to the nano–particle by its interaction with SWs results in a huge kick when compared to that provided by the photon. Such is the case of the pulling force, a force that pull the particle in the opposite direction as that of the incident photons, exerted on dielectric nano–particles placed near a metallic interface arising from the excitation of metallic SWs [2,3].

Possibilities have been broadened with the advent of metamaterials, synthetic composite material exhibiting electromagnetic properties not usually found in natural materials, where new optomechanics effects, as light induced levitation or strong optical pulling forces achievement, have been demonstrated [4–6]. In particular, transparent metamaterials with negative index of refraction (NIR) at the low–frequency spectrum, *i.e.*, both permittivity and permeability with a negative real part in the terahertz (THz) and infrared (IR) region, have expanded the possibilities of having SWs not only with *p* but also with *s* polarization at these frequency ranges. In particular, NIR materials have stimulated a revived interest in the electromagnetic properties of SWs, and

#515221 https://doi.org/10.1364/OPTCON.515221
Journal © 2024 Received 5 Dec 2023; revised 13 Feb 2024; accepted 15 Feb 2024; published 13 Mar 2024

OPTICS CONTINUUM

novel characteristics that do not exist in conventional media, such as backward behavior, with a total energy flux parallel to the interface, that is opposed to the phase velocity, have been reported in several works [7,8]. This property has been recently harnessed for optical surface tractor beams employing NIR materials [9].

In the present work, we propose the theoretical idea of a single localized defect on a plane NIR interface working as a source that is able to provide optical pulling or pushing force on dielectric nano–particles placed near the NRI interface. Interestingly, in case of the pulling source, the mechanism for which the particles are moved in the source direction in the present work is different from that used in Refs. [2,10,11], where the pulling force arises from the interaction between the circularly polarized dipolar moment induced on the nano–particle and the surface modes on the surface which can be excited by the near field scattering [12]. On the contrary, here, the direction of the force towards the source results by the electromagnetic pressure exerted on the nano–particle placed into the dielectric medium (vacuum in our simulations) and the excitation of backward SWs on the surface.

2. Theory

In order to demonstrate the above, we consider a localized defect with translation symmetry along an axis (the y axis in our coordinate system) which scatters the impinging light on the flat NRI surface containing the defect (Fig. 1). The medium above the surface, where the dielectric nano–particles are placed, is vacuum ($\varepsilon_1 = \mu_1 = 1$) and the constitutive parameters of the NRI medium are ε_2 and μ_2, both with negative real part. The illumination is fulfilled by a Gaussian beam which is pointing in the direction of the center of the surface defect, $x = z = 0$ in our coordinate system, $\phi_i(x,z) = e^{-(x\cos\phi_0 + z\sin\phi_0)^2/w^2} e^{ik_0(x\sin\phi_0 - z\cos\phi_0)}$, where $\phi_i(x,z)$ is the y–directed component of the total magnetic field (p polarization) or the total electric field (s polarization), w is half of the beam width at the waist, ϕ_0 is the angle of incidence of the beam defined with respect to the z axis, ω is the angular frequency and c is the speed of light in vacuum. The solution $\phi(x,z)$ of Maxwell's equations in the region $z>h$ can be written as

$$\phi(x,z) = \phi_i(x,z) + \int_{-\infty}^{+\infty} R(\kappa)\, e^{ik_0\kappa x + i\beta^{(1)} z} d\kappa, \tag{1}$$

where κ is the normalized to the photon wave–vector in vacuum $k_0 = \omega/c$, $\beta^{(1)} = k_0\sqrt{1-\kappa^2}$, ω is the angular frequency, c is the vacuum speed of light and R is the complex amplitude of the field obtained from the surface values of the total field and its normal derivative (See Supplement 1, Section 1 and 2). Under suitable conditions, the near field scattering generates SWs carrying energy far away from the defect, on $\pm x$ directions in our coordinate system. Then, a dielectric nano–particle placed close to the interface can be pushed away from the defect or towards it. In the first case, the defect behaves as a pushing source whereas, in the second case the defect behaves as a pulling or tractor source. Pushing sources are commonly established by the use of conventional scatter objects, where the scattered light carries momentum (and energy) propagating away from the object. Although SWs can be excited by a variety of incident beams, we have focused on a beam of finite width (a Gaussian beam in our case), rather than a plane wave, impinging on the NRI boundary. In addition to approximate more closely experimental situations, the use of a finite width beam has a numerical advantage: the field values on the surface separating two media far enough from the protuberance can be considered as zero and, consequently, this portion of the surface does not contribute to the scattering field [13].

The novelty of this work is the theoretical demonstration of a tractor source, for which the momentum and energy carried by the scattered light in vacuum points out towards the object. To achieve this situation, and in order to avoid an energy sink at the position of the object (the surface defect in this work), it is necessary to have another channel where the energy flows in the

OPTICS CONTINUUM

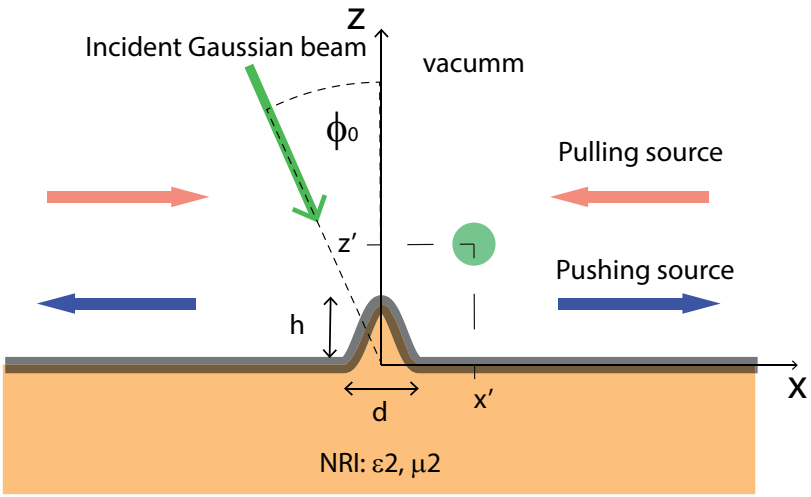

Fig. 1. Scheme of the pushing/pulling defect source system. The medium above the interface is vacuum ($\varepsilon_1 = \mu_1 = 1$) and the constitutive parameters of the NRI medium are ε_2 and μ_2, both with a negative real part. A Gaussian beam of half–width w impinges from the upper medium with an angle of incidence ϕ_0 which specifies the inclination of the beam with respect the z axis. A dielectric nano–particle placed at position $\mathbf{r'} = x'\hat{x} + y'\hat{y}$ can be pushed far away from the defect source or towards it. The arrows indicate the direction of the optical force.

opposite direction, *i.e.*, away from the object and such that the nano–particle cannot access to it. This is the scheme proposed in the present work.

In our calculations, we have considered two kind of metamaterial boundaries, one of them supporting p–polarized forward SWs and the other p–polarized backward SWs. For clarity, we have chosen the NRI constitutive parameters so that the phase velocity of forward and backward SWs aproximately match. In the first case (case I), $\varepsilon_2 = -1.3 + i0.01$, $\mu_2 = -0.35 + i0.01$, which leads to a normalized propagation constant $\kappa_{sw} = k_x/k_0 = 1.337 + i0.02$. In the second case (case II), $\varepsilon_2 = -0.8 + i0.01$, $\mu_2 = -1.6 + i0.01$, which leads to a normalized propagation constant $\kappa_{sw} = 1.332 - i0.0379$. Note that in the first case the sign of the imaginary part of the propagation constant is equal to that of the real part, meaning that the SW phase velocity is in the same direction as the energy flow (forward SW). On the contrary, in the second case, the sign of $\Im\, \kappa_{sw}$ is opposed to that of the $\Re\, \kappa_{sw}$, meaning that the phase velocity is in the opposed direction as the energy flow (backward SW).

3. Results

In order to find the value of the force acting on the nano–particle along the x axis, we assume that the radius a of the particle is smaller than SW and photon wavelengths, $a \ll \lambda_{sw} = \lambda/\Re\, \kappa \approx \lambda/1.3$ (the photon wavelength in vacuum is $\lambda = 2\pi c/\omega$). In this framework, the time average of the force acting on a single particle located at the position $\mathbf{r}$ is written as [14],

$$F_x(\mathbf{r}) = \frac{1}{2}\mathrm{Re}\sum_{j=x,y,z} p_j^* \frac{\partial}{\partial x} E_j(\mathbf{r}) \approx \frac{1}{2}\mathrm{Re}\left[\alpha_0^* \sum_{j=x,z} E_j^*(\mathbf{r}) \frac{\partial}{\partial x} E_j(\mathbf{r})\right] \tag{2}$$

where E_j is the j component of the electric field, $\mathbf{p}$ is the induced electric dipole on particle. In the last equality, we have used the fact that the dipole moment $\mathbf{p} \approx \alpha_0\, \mathbf{E}$, where $\alpha_0 = \frac{\alpha_e}{1 - i\frac{k_0^3}{6\pi\varepsilon_0}\alpha_e}$ is

OPTICS CONTINUUM

the nano–particle polarizability in vacuum ($\alpha_e = 4\pi\varepsilon_0\, a^3 \frac{\varepsilon_p - 1}{\varepsilon_p + 2}$), and the fact that the y component of the electric field is null.

In all the examples presented here we have calculated the normalized force with respect to the electromagnetic pressure on the same nano–particle exerted by a plane wave propagating along the x direction whose amplitude coincides with that of the Gaussian beam at the center of it, *i.e.*, $f = F_x/F_{ph}$ where $F_{ph} = 0.5\, k_0\, \Im\alpha_0\, |\mathbf{E}_{ph}|^2$, $\mathbf{E}_{ph} = \sqrt{\frac{\mu_0}{\varepsilon_0}}\phi_{inc}(0,0)\, e^{i\, k_0\, x}\, \hat{z}$ and ε_0, μ_0 are the vacuum permittivity and permeability, respectively.

In Fig. 2 we have plotted the dependence on the x axis of the normalized optical force f exerted on a dielectric nano–particle (radius $a = 0.01\lambda$ and dielectric permittivity $\varepsilon_p = 2.25$) near the surface with a protuberance $g(x) = \mathrm{rec}(x/d)\, h\, [1 + \cos(2\pi\, x/d)]$ ($\mathrm{rec}(u)$ is the rectangular function centered at the origin with unit width and height), which represent the pulling or pushing source, with $d = \lambda$ and height $h = 0.125\lambda$. The vertical position of the particle has been set at $z' = 0.125\lambda$ and $z' = 0.250\lambda$. The illumination is accomplished by a Gaussian beam of width $w = 5\lambda$. In case I, corresponding to the excitation of forward SWs, the force has the same sign as the x axis, *i.e.*, $F_x{>}0$ for $x{>}0$ and $F_x{<}0$ for $x{<}0$. This fact means that the protuberance behaves as a pushing source. We observe that the force curve has a periodic behavior along the x axis with a period $\Lambda = 0.77\lambda$ gradually attenuating with the increasing distance $|x|$, with a decay length $\delta \approx 8\lambda$. The value of the period coincides with that of the SW wavelength $\lambda_{sw} = \lambda/\kappa_{sw} \approx 0.76\lambda$, whereas the decay length coincides with that of the SW, $\delta = \lambda/(2\pi\, \Im\, \kappa) \approx 7.95\lambda$. These facts make clear that the main contribution to the optical force pushing the nano–particle away from the protuberance is due to the SW field.

On the other hand, from Fig. 2 we see that for case II, corresponding to backward SWs excitation, the optical calculation force values are negative (positive) for $x{>}0$ ($x{<}0$). This fact can be understood by taking into account the fact that in backward SWs the sign of the real part of the propagation constant is opposite to the corresponding imaginary part. As a consequence, the energy carried by the backward SW is opposite to its direction of propagation. As the energy must attenuate, the exponential SW decay is in the same direction as the total energy flow, that is, the imaginary part of the propagation constant must be positive for $x{>}0$ and negative for $x{<}0$. Therefore, for $x{>}0$ is $\Re\, \kappa_{sw}{<}0$, and for $x{<}0$ is $\Re\, \kappa_{sw}{>}0$. From the above discussion it follows that the SW field pushes the nano–particle towards the protuberance behaving as a tractor source. The force curves also show a periodic spatial dependence along the x–direction, $\Lambda = \lambda/\Re\, \kappa_{sw} \approx 0.75\lambda$ gradually attenuating with the increase of $|x|$, with a decay length $\delta = \lambda/(2\pi\, \Im\kappa_{sw}) \approx 4.2\lambda$ owing to losses arising from absorption in the NRI medium.

In addition, in Fig. 2 (inset at the right side) we have plotted the modulus of the complex reflection coefficient $|R|$ as a function of the normalized wave–vector κ. In the radiative zone, $|\kappa|{<}1$, the curves show a central peak at $\kappa = 0$ representing the wave reflected by the planar interface (without the protuberance). The protuberance is manifested by the presence of the peaks outside the radiative zone, $|\kappa|{>}1$. These peaks are centered at $\kappa \approx \pm 1.3$ and represent the SWs excited by the scattering of the incident field with the protuberance.

To add a physical insight, one can estimate quantitatively the SW component of the optical force as follows. Since the main contribution to the integral (1) is provided by the SW excitation (see inset at the right in Fig. 2), it follows that the near field can be approached by their contributions. To do this, one should take into account the forward or backward character of the excited SW since physical causality requires the attenuation of the field as $|x| \longrightarrow \infty$. From the above discussion, it follows that for $x{>}0$, the SW field can be approximately by the following expression,

$$\phi(x,z) = A(\kappa_{sw})\, e^{ik_0\kappa_{sw}x + i\beta^{(1)}(\kappa_{sw})z} \tag{3}$$

for forward SW excitation, whereas for backward SW excitation is,

$$\phi(x,z) = A(\kappa_{sw})\, e^{-ik_0\kappa_{sw}x + i\beta^{(1)}(-\kappa_{sw})z}, \tag{4}$$

OPTICS CONTINUUM

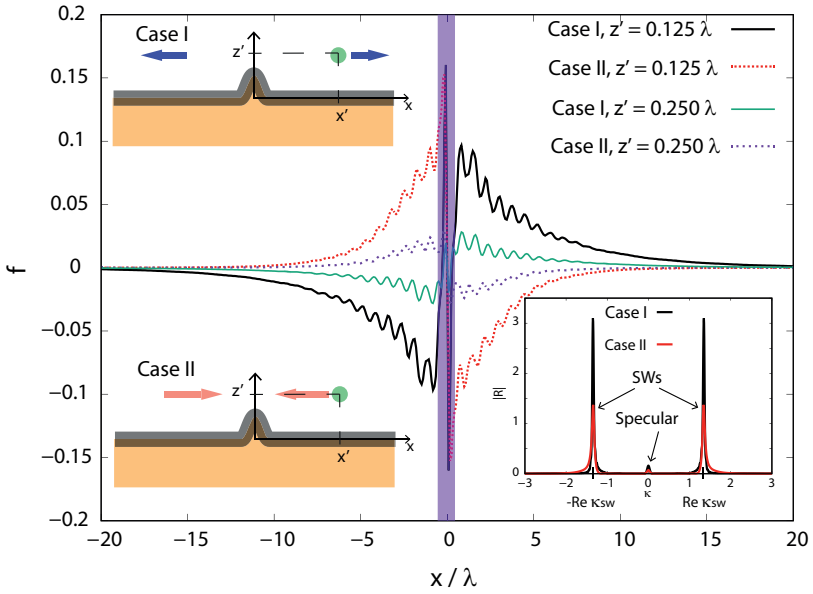

Fig. 2. Optical force as a function of the x coordinate of the particle for $z' = 0.125\lambda$ and $z' = 0.250\lambda$. Case I: $\varepsilon_2 = -1.3 + i0.01$, $\mu_2 = -0.35 + i0.01$ (forward SW excitation), and case II: $\varepsilon_2 = -0.8 + i0.01$, $\mu_2 = -1.6 + i0.01$ (backward SW excitation). The vertical segment in blue have a width λ indicating the width d of the protuberance. Insets at the left show the pushing (above) and pulling (bottom) behavior of the protuberance for the cases I and II, respectively. Inset at the right side shows the modulus of the reflection coefficient as a function of the normalized wave–vector κ. The half of the beam width $w = 5\lambda$. The arrows indicate the direction of the optical force.

where $A(\kappa_{sw})$ can be calculated as $2\pi i$ times the residue of the complex amplitude R, $\lim_{\kappa \longrightarrow \kappa_{sw}}(\kappa - \kappa_{sw})\, R(\kappa)$, or by integrating Eq. (1) into a bandwidth $\Re\,\kappa$ that embraces the whole resonant peak, *i.e.*, $A = \int_{\Re\,\kappa_{sw}-\Delta_\kappa/2}^{\Re\,\kappa_{sw}+\Delta_\kappa/2} R(\kappa)\, d\kappa$ with Δ_κ embracing the resonant peak at $\pm\Re\kappa_{sw}$ [12,15]. From Eqs. (3), (4) and Maxwell–Ampere, we calculate the electric field $\mathbf{E}_{sw}$ and deduce an expression for the SW contribution to the optical force (2) for x>0,

$$F_{sw}(\mathbf{r}) = \frac{k_0}{2}\mathrm{Re}\left[\pm i\kappa_{sw}\,\alpha_0^*\,|\mathbf{E}_{sw}|^2\right] \approx \pm\frac{k_0}{2}\,\Im\{\alpha_0\}\,\kappa_{sw}|\mathbf{E}_{sw}|^2, \tag{5}$$

where the positive (negative) sign corresponds to forward (backward) excited SW. In the last equality in Eq. (5) we have used the fact that the SW propagation constant is almost a real number. From Eq. (5) we can see that the optical force exerted on the nano–particle placed at position with x>0 is in the $+x$ ($-x$) direction for forward (backward) SW excitation. Note that we have to change $\kappa_{sw} \longleftrightarrow -\kappa_{sw}$ in Eqs. (3), (4) and (5) for x<0.

In Fig. 3 we have plotted the optical force (2) for various values of the half of the beam width, $w = 5\lambda, 2.5\lambda, \lambda$ together with the SW contribution calculated with Eq. (5). We observe that the spatial variations on these curves are appreciable in the interval defined from $-w$ to w. This fact is due to the interference process between the specular reflected beam and the SWs excited by the near field scattered by the protuberance. We also observe that the SW contribution curve falls in the middle of the oscillation of those corresponding to the total force calculated with our rigorous integral method. Similar results, not showed here, have been obtained for the forward SWs excitation.

OPTICS CONTINUUM

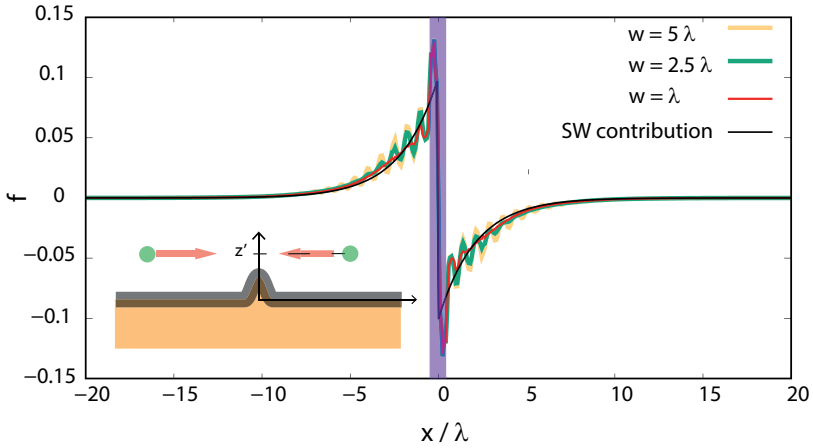

Fig. 3. Normalized force f as a function of the x coordinate for backward (case II) SW excitation and for various values of the half of the beam width, $w = 5\lambda,\ 2.5\lambda,\ \lambda$. The particle is placed at $z' = 0.125\lambda$. We have included the SW contribution to the normalized force f calculated using Eq. (5). All other parameters are the same as in Fig. 2. The inset illustrates the pulling behavior of the protuberance.

Next, we study the dependence with the angle of incidence ϕ. From Fig. 4(a) and 4(b) we see that for forward (backward) SWs excitation, the force values are increased for $x>0$ ($x<0$) as the angle of incidence is increased. In addition, the force values are remarkably reduced in the opposite side, *i.e.*, on the $x<0$ region for forward SW excitation and on $x>0$ region for backward SW excitation. This fact can be understood by means of the reflectivity plots shown in Fig. 4(c) and 4(d), where we see that the amplitude $R(\Re\kappa_{sw})$ increases with the increment of ϕ, whereas the amplitude $R(-\Re\kappa_{sw})$ decreases with ϕ, thus, the excited SWs with propagation constant $+\kappa_{sw}$ are strongly excited with respect to that with $-\kappa_{sw}$. As a consequence, from Eqs. (3) and (4) we see that the near field, and thus the SW contribution to the optical force (5), are increased on the right side $x>0$ for forward SW excitation and on left side $x<0$ for backward SW excitation. We also observe an asymmetry, which is more noticeable as the angle of incidence increases, in the period of the optical force at both sides of the protuberance. The occurrence of this asymmetry arise in the interference between the incident (and reflected field) and the SWs excited in the process [8]. The period can be roughly estimated in the limit of planar wave incidence, *i.e.*, by assuming an incident plane wave ($w = \infty$) with wave–vector component parallel to the interface $k_{inc} = k_0 \sin\phi_0$. Therefore, since the angle of incidence is grater than zero, $\phi_0>0$, the periods of the near field at both sides of the protuberance, for forward SW excitation, are $d_> = 2\pi/|k_{inc} - k_0\kappa_{sw}| = \lambda/|\sin\phi_0 - \kappa_{sw}|$ for $x>0$ and $d_< = 2\pi/|\sin\phi_0 + \kappa_{sw}|$ for $x<0$. On the contrary, for backward SW excitation, the periods are: $d_> = 2\pi/|\sin\phi_0 + \kappa_{sw}|$ for $x>0$ and $d_< = 2\pi/|\sin\phi_0 - \kappa_{sw}|$ for $x<0$. For example, for backward SW excitation, from Fig. 4 we obtain $d_< \approx 0.772\lambda,\ 0.926\lambda,\ 1.112\lambda$ for $\phi = 5,\ 15,\ 30°$, respectively, whereas the corresponding calculated values are: $d_< \approx 0.803\lambda,\ 0.9318\lambda,\ 1.201\lambda$. We have verified, not shown here, that the calculated values using the plane wave incidence limit converge to those rigorously obtained for values large enough of half beam width w ($w>10\lambda$).

OPTICS CONTINUUM

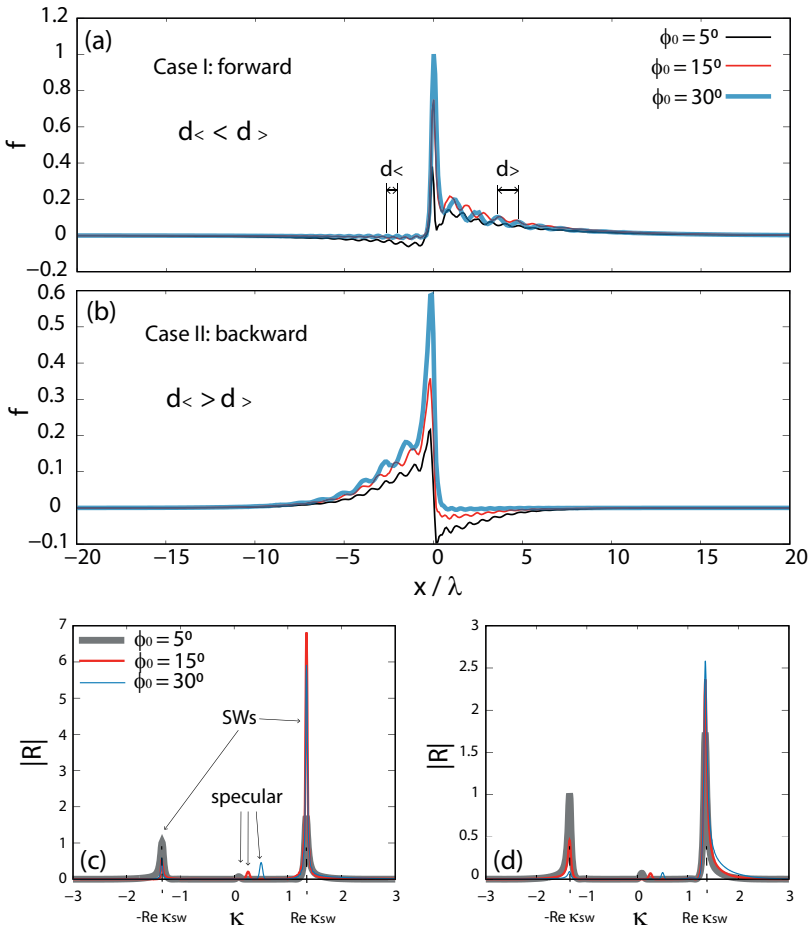

Fig. 4. Optical force as a function of the x coordinate for several incidences angles for the cases in which forward (a) and backward (b) SWs are excited. The particle is placed at $z' = 0.125\lambda$. Reflectivity $|R|$ as a function of the normalized to the photon wave–vector κ for forward (case I) (c) and backward (case II) (d) SW excitation. Both the specular reflection and amplitude of the SWs field are indicated by arrows. All other parameters are the same as in Fig. 2.

OPTICS CONTINUUM

4. Conclusion

In conclusion, we have analyzed the scattering process for which a metamaterial planar boundary including a sub–wavelength protuberance behaves like a pushing or pulling beam source. Our results shown that the main character in this phenomenon are the SWs existing on the metamaterial boundary and their dynamic characteristics that provide the pulling or pushing optical force. By modifying the angle and the width of the incidence Gaussian beam, one can handle the force level at both sides of the protuberance and the spatial length of the fluctuation due to the interference between the reflected field by the plane metamaterial boundary (without any defect) and the SW generated by the scattering of the near field with the protuberance. The knowledge developed in this work could be interesting towards the development of pulling beam sources based on surface waves excitation.

Funding. School of Engineering of Universidad Austral (O04-INV0 0 020).

Acknowledgments. We acknowledge the financial supports of Universidad Austral O04-INV0 0 020, Agencia Nacional de Promoción de la Investigación, el desarrollo Tecnológico y la Innovación PICT-2020-SERIEA-02978 and Consejo Nacional de Investigaciones Científicas y Técnicas (CONICET).

Disclosures. The authors declare no conflicts of interest.

Data availability. Data underlying the results presented in this paper are not publicly available at this time but may be obtained from the authors upon reasonable request.

Supplemental document. See Supplement 1 for supporting content.

References

1. S. Maier, Plasmonics: Fundamentals and Applications (Springer-Verlag, New York, 2007).
2. M. I. Petrov, S. V. Sukhov, A. A. Bogdanov, *et al.*, "Surface plasmon polariton assisted optical pulling force," Laser & Photonics Reviews **10**(1), 116–122 (2016).
3. H. Ferrari, V. Herrero, and M. Cuevas, "Optical pulling force on dielectric particles via metallic slab surface plasmon excitation: a comparison between transmission and reflection schemes," Opt. Lett. **48**(9), 2345–2348 (2023).
4. Y. Kiasat, M. G. Donato, M. Hinczewski, *et al.*, "Epsilon-near-zero (enz)-based optomechanics," Commun. Phys. **6**(1), 69 (2023).
5. F. J. Rodriguez-Fortuno and A. V. Zayats, "Repulsion of polarised particles from anisotropic materials with a near-zero permittivity component," Light: Sci. Appl. **5**(1), e16022 (2016).
6. A. Ivinskaya, N. Kostina, N. Proskurin, *et al.*, "Optomechanical manipulation with hyperbolic metasurfaces," ACS Photonics **5**(11), 4371–4377 (2018).
7. S. A. Darmanyan, M. Nevi'ere, and A. A. Zakhidov, "urface modes at the interface of conventional and left-handed media," Opt. Commun. **225**(4-6), 233–240 (2003).
8. M. Cuevas, V. Grunhut, and R. A. Depine, "Near field evidence of backward surface plasmon polaritons on negative index material boundaries," Phys. Lett. A **380**(47), 4018–4021 (2016).
9. N. Wang and J. N. G. G. Wang, "Morphology-independent general-purpose optical surface tractor beam," Research Square, rs.3.rs-3386776/v1 (2023).
10. H. Ferrari, C. J. Zapata-Rodríguez, and M. Cuevas, "Graphene plasmons on attenuated total reflection structures: a route to achieve large optical pusshing or pulling force intensities in the terahertz region," J. Opt. Soc. Am. B **39**(12), 3200–3208 (2022).
11. H. Ferrari, C. J. Zapata-Rodríguez, and M. Cuevas, "Giant terahertz pulling force within an evanescent field induced by asymmetric wave coupling into radiative and bound modes," Opt. Lett. **47**(17), 4500–4503 (2022).
12. F. Rodríguez-Fortuno, A. M. N. Engheta, and A. Zayats, "Lateral forces on circularly polarizable particles near a surface," Nat. Commun. **6**(1), 8799 (2015).
13. A. Maradudin and E. Mendez, "Light scattering from randomly rough surfaces," Science Progress **90**(4), 161–221 (2007).
14. P. Chaumet and M. Nieto-Vesperinas, "Time-averaged total force on a dipolar sphere in an electromagnetic field," Opt. Lett. **25**(15), 1065–1067 (2000).
15. J. Olivo, C. Zapata-Rodríguez, and M. Cuevas, "Spatial modulation of the electromagnetic energy transfer by excitation of graphene waveguide surface plasmons," J. Opt. **21**(4), 045002 (2019).